Published in final edited form as:
J Biomed Mater Res A. 2011 February ; 96(2): 436–448. doi:10.1002/jbm.a.32997.

In vivo performance of a phospholipid-coated bioerodable elastomeric graft for small-diameter vascular applications

Lorenzo Soletti[1,2,3,4], **Alejandro Nieponice**[1,3,4], **Yi Hong**[1,3,4], **Sang-Ho Ye**[1,3,4], **John J. Stankus**[3,5], **William R. Wagner**[1,2,3,4,5], and **David A. Vorp**[1,2,3,4,*]

[1]Department of Surgery, University of Pittsburgh, Pittsburgh, Pennsylvania 15219

[2]Department of Bioengineering, University of Pittsburgh, Pittsburgh, Pennsylvania 15219

[3]McGowan Institute for Regenerative Medicine, University of Pittsburgh, Pittsburgh, Pennsylvania 15219

[4]Center for Vascular Remodeling and Regeneration, University of Pittsburgh, Pittsburgh, Pennsylvania 15219

[5]Department of Chemical Engineering, University of Pittsburgh, Pittsburgh, Pennsylvania 15219

Abstract

There remains a great need for vascular substitutes for small-diameter applications. The use of an elastomeric biodegradable material, enabling acute antithrombogenicity and long-term in vivo remodeling, could be beneficial for this purpose. Conduits (1.3 mm internal diameter) were obtained by electrospinning biodegradable poly(ester urethane)urea (PEUU), and by luminally immobilizing a non-thrombogenic, 2-methacryloyloxyethyl phosphorylcholine (MPC) copolymer. Platelet adhesion was characterized in vitro after contact with ovine blood. The conduits were implanted as aortic interposition grafts in the rat for 4, 8, 12, and 24 weeks. Surface treatment resulted in a 10-fold decrease in platelet adhesion compared to untreated material. Patency at 8 weeks was 92% for the coated grafts compared to 40% for the non-coated grafts. Histology at 8 and 12 weeks demonstrated formation of cellularized neotissue consisting of aligned collagen and elastin. The lumen of the grafts was confluent with cells qualitatively aligned in the direction of blood flow. Immunohistochemistry suggested the presence of smooth muscle cells in the medial layer of the neotissue and endothelial cells lining the lumen. Mechanically, the grafts were less compliant than rat aortas prior to implantation ($4.5 \pm 2.0 \times 10–4$ mmHg–1 vs. $14.2 \pm 1.1 \times 10–4$ mmHg–1, respectively), then after 4 weeks in vivo they approximated native values, but subsequently became stiffer again at later time points. The novel coated grafts exhibited promising antithrombogenic and mechanical properties for small-diameter arterial revascularization. Further evaluation in vivo will be required to demonstrate complete remodeling of the graft into a native-like artery.

Introduction

Despite the clinical need for small diameter (<6 mm) vascular bypass grafts for arterial cardiac or peripheral revascularization, the standard of care remains the use of autologous blood vessels. Such procedures rely on the use of healthy autologous arteries or veins (in those cases requiring more than one graft). Neither of these native vessels are ideal

*Correspondence: David A. Vorp, Department of Surgery, University of Pittsburgh, Pittsburgh, Pennsylvania 15219, David A. Vorp (VorpDA@upmc.edu).

substitutes as they have limited availability, suboptimal performance, and are associated with donor-site morbidity [1].

Commercially available, biodurable vascular grafts, while routinely used for large-diameter applications, have invariantly failed for small diameter cases due to thrombogenicity at the blood-material interface and mechanical mismatch with the host artery, both of which accelerate the two aforementioned modalities of graft failure [2]. Efforts have been dedicated, throughout the past several decades, to develop implantable biomaterials for tissue engineering approaches that could provide a temporary biodegradable support to at least acutely meet the mechanical and functional demand of the target tissue, while gradually degrading to allow *in situ* native tissue regeneration.

Several attempts have been made to produce a successful biodegradable scaffold material for vascular tissue engineering using both biological (*e.g.*, decellularized native tissues [3, 4], biological proteins [5], hydrogels [6]), synthetic materials (*e.g.*, polyesters [7, 8], and polyurethanes [9, 10]). While each of the previous methods have their merits, to date there is no clear consensus as to what approach – past, present, or future – might lead to a clinically-applicable treatment. Potential limitations toward clinical translation include the lack of off-the-shelf availability [11], lack of appropriate mechanical property matching to native arteries, which could lead to rupture or aneurysm formation in case of insufficient strength [12], or graft obstruction due to compliance mismatch [13], host tissue inflammation due to acidic scaffold degradation products [14], and thrombogenicity [15]. Targeted surface modification of materials for vascular applications with either functional polypeptid groups (*e.g.*, cell adhesive ligands [16]), antithrombogenic proteins (*e.g.*, heparin [17]), or cell monolayers (*e.g.*, endothelial cells [18]) have been made in an attempt to improve scaffold antithrombogenic properties. Recently, bioinspired phospholipid polymers and co-polymers based on 2-methacryloyloxyethyl phosphorylcholine (MPC) have been successfully used to reduce platelet adhesion on blood-contacting surfaces [19, 20].

In this study we tested the *in vivo* performance of a small-diameter vascular graft made with a previously described biodegradable and cytocompatible poly(ester urethane) urea (PEUU) processed by electrospinning [21]. Electrospun PEUU (ES-PEUU) has been shown to possess mechanical properties remarkably similar to native arteries [22]. The scaffolds were luminally coated with an MPC-based copolymer layer in an attempt to create a non-thrombogenic surface, and implanted for up to 24 weeks as abdominal aortic interposition grafts in a rat model.

Materials and Methods

PEUU synthesis

Polycaprolactone diol (PCL, Mn=2000, Sigma) was dried under vacuum for 48 h at 50°C. Putrescine (Sigma) and 1,4-diisocyanatobutane (BDI, Sigma) were distilled under vacuum. Stannous octoate (Sigma) catalyst was dried using 4Å molecular sieve. 1,1,1,3,3,3-hexafluoroisopropanol (HFIP, Oakwood) and dimethyl sulfoxide (DMSO, Sigma) were used as received. PEUU was synthesized from BDI and PCL with putrescine chain extension as described previously [23]. Synthesis proceeded as a solution polymerization with DMSO using a 2:1:1 BDI:PCL:putrescine molar ratio.

ES-PEUU scaffold preparation

The ES-PEUU conduits were fabricated using an electrospinning apparatus and technique previously described [21]. Briefly, PEUU solution in HFIP (8% w/w) was prepared and loaded into 10 mL syringes connected by plastic tubing to a stainless steel capillary (ID=1.2 mm), which was suspended 14 cm over a stainless steel mandrel (diameter=1.3 mm). The

mandrel was rotated at 250 rpm and simultaneously translated on an x-y stage (Velmex Inc., Bloomfield, NY) along the longitudinal direction of the mandrel in a cyclic manner (translational speed=6 cm/s, amplitude=8 cm, frequency=0.4 Hz). The mandrel was charged at −10 kV, while the capillary was charged with 10 kV. High voltage was supplied for each component using a combination of two high voltage generators (Gamma High Voltage Research, Ormond Beach, FL). The polymer solution was infused with a precision syringe pump (Harvard Apparatus, Holliston, MA) at 1 mL/h, and an electrospinning time of 15 min.

At the end of the process, electrospun polymer that had deposited beyond the extension of the central 10 cm of scaffold was removed with a razor and the scaffolds were then slid out of the mandrel and were dried within a vacuum chamber for 24 h.

ES-PEUU surface modification with phospholipid copolymer

A phospholipid copolymer (PMA) comprised of 70 mol% MPC and 30 mol% methylacrylic acid (MA; Mw=5.5×10^5) synthesized by the conventional radical polymerization [24] was kindly provided from Dr. Kazuhiko Ishihara (University of Tokyo, Tokyo, Japan).

ES-PEUU scaffold surfaces were pre-treated by ammonia plasma using radio frequency glow discharge (RFGD, MARCH GCM250, March Instrument Inc, CA). The plasma power applied was 25 W, at a frequency of 13.65 MHz for 2 min under 0.6 mTorr pressure. The resulting surface-aminated PEUU scaffolds were subsequently immersed in 0.25 wt% PMA copolymer solution in water and a condensation reagent was added ((1-ethyl 3-(3-dimethylaminopropyl) carbodiimide) hydrochloride, EDC, [EDC]/[PMA] = 50). The PMA solution was in contact with the scaffolds surfaces for 24 h at 37°C within a rocking platform. The PMA was chemically immobilized on the surface through the reaction between the carboxyl groups in the PMA and the amine groups on the ES-PEUU surface. After modification with PMA, scaffold samples were washed 5 times with deionized water and dried under vacuum. A schematic of the surface modification process is shown in Fig. 1. The scaffolds were sterilized by immersion in 70% ethanol solution for 24 h followed by multiple washes with sterile Dulbecco's modified phosphate buffered saline (DPBS).

Morphological assessment

ES-PEUU scaffolds were immersed in liquid nitrogen and rapidly cut with a cold razor to generate a sharp fracture, exposing a cross-section with preserved structural features. The specimens were mounted dry on aluminium stubs with a double adhesive copper tape and sputter coated with a 3.5 nm thick layer of gold/palladium (Sputter Coater 108 auto, Cressington Scientific Instruments Inc., Cranberry Twp., PA). The cross-sections were imaged by field emission scanning electron microscopy (SEM) (JSM-6330F, JEOL USA, Inc., Peabody, MA).

In vitro platelet adhesion assessment

Whole ovine blood was collected from healthy animals and immediately added to monovette tubes containing 0.3 mL of 0.106 M trisodium citrate (Sarstedt, Newton, NC). PMA-modified (n=5) or unmodified ES-PEUU (n=5) scaffolds were placed into BD Vacutainer® tubes containing 5 mL citrated ovine blood and incubated for 4 h under continuous rocking. The surfaces were then rinsed with PBS and immersed in a 2.5% glutaraldehyde solution for 2 h at 4°C to fix the deposited platelets, the samples were then washed 3 times in PBS (15 min each), treated for 1 h in 1% (w/v) OsO_4 solution and washed 3 more times with PBS. Samples were then serially dehydrated with increasing ethanol solutions and critical point dried (Emscope CPD 750, Emscope Lab., Ashford, UK) with 4 cycles of liquid CO_2 soaking and venting at 10°C before reaching the critical point for CO_2 at 31.1°C at 1100 psi.

Samples were subsequently mounted on aluminium stubs, sputter coated with gold/palladium, and observed using SEM as previously described.

The density of platelet deposition on the surface of the scaffolds following exposure to ovine blood was quantified using an image-based technique. Briefly, a set of images depicting 5 random fields of view of each specimen was taken for each of the two groups (PMA-modified and unmodified ES-PEUU scaffolds). A mask of determined area (quantified using ImageJ software) was randomly applied to 5 different locations within each SEM image. The number of adhered platelets within the applied mask was counted manually and the average between the two groups was compared.

Mechanical properties

Dynamic compliance measurements were performed using a previously described vascular perfusion system [25] using previously described methods [26]. Briefly, a Biomedicus centrifugal pump (Biomedicus 520D, Medtronic, Minneapolis, MN) delivered saline at 37°C under sinusoidal (pulsatile) intraluminal pressure and flow consistent with physiologic values (120/80 mmHg and 100 mL/min, respectively) to the specimen. The intraluminal pressure was measured by proximal and distal transducers (TruWave, Edward Lifesciences, Irvine, CA) and the outer diameter of the tubular specimen was measured with a He-Ne laser micrometer (Beta LaserMike, Dayton, OH). Both pressure and diameter signals were automatically recorded at 30 Hz over 1 min once per hour over 24 hours by an acquisition card connected to a personal computer. Dynamic compliance, C, was calculated from recordings of pressure, P and diameter, D_p as:

$$C=\frac{(D_{120}-D_{80})}{D_{80}}\frac{1}{P_{120}-P_{80}} \quad (1)$$

Where P_{120}=120 mmHg and P_{80}=80 mmHg, and D_{80} and D_{120} were the diameters corresponding to P_{80} and P_{120}, respectively.

To measure uniaxial material properties of the conduits, a ring of each specimen was cut (~1 mm width) and measured for diameter, thickness, and width using a digital caliper (Fisher-Scientific). The rings were then mounted in a uniaxial tensile testing system (Series 1101, Applied Test Systems Inc., Butler, PA) using a 10 lb force transducer (SM-10, Interface, Scottsdale, AZ), which was modified to perform the testing in physiologic saline at 37°C, as previously described [22]. Load–displacement curves were computed to obtain Cauchy stress–stretch relationships. Ultimate tensile stress and stretch to failure were taken as, respectively the maximum stress value before failure and its corresponding value of stretch.

Abdominal aortic interposition graft placement in the rat

All procedures involving animals were approved by the University of Pittsburgh's Institutional Animal Care and Use Committee. Adult Lewis rats (Charles River Laboratories, Boston, MA) with a weight range of 200–300 grams were used. Anaesthesia was induced with 3% isofluorane inhalation and maintained with 1% isofluorane and 50 mg/kg ketamine administered via intraperitoneal injection. The surgery was performed with the rat in supine position placed on a warming pad. The anterior abdominal wall was shaved and aseptically prepared with povidone-iodine. The abdominal aorta was exposed by a midline laparotomy incision and displacement of the viscera with a retractor. The aorta was carefully separated from the vena cava and clamped in proximity to the renal arteries and the iliac bifurcation with microvascular clamps to maintain the original *in vivo* length. Prior to clamping, a dose of 40 IU of heparin was administered intravenously through a tributary to the vena cava. A 1 cm aortic gap was created and grafted with either ES-PEUU (n=25) or

PMA-coated ES-PEUU (n=12) scaffolds. The anastomoses were made in an end-to-end fashion to the native aorta with 5 or 6 separate stitches using 10-0 Prolene (Ethicon) under 10× magnification (M691, Wild-Heerbrugg). The muscle layer and the skin were closed with 3-0 Vicryl™ absorbable suture. A povidone-iodine ointment was applied on the sutured abdominal incision at the end of the procedure to prevent infection. Standard analgesic and antibiotic therapy was administered following the surgery. Aspirin was administered daily (100 mg/day/kg).

Fluoroscopy

At the end of the designated implant times, animals were sacrificed by a lethal intracardiac injection of KCl mixed with heparin (1000 units) solution while under deep anaesthesia (5% isofluorane). The thoracic descending aorta was immediately exposed by displacing the heart and lungs and cannulated with a 22G Angiocath (Becton Dickinson, Sandy, UT) secured with a 4-0 silk ligation. The animal was placed under an angiography system (OEC 9800 Plus, GE Healthcare, Piscataway, NJ) and iodine contrast media (Renografin-60, Bracco Diagnostics, Princeton, NJ) was manually infused through the angiocath during irradiation to assess graft patency. Patency rate was calculated at 8 weeks as the ratio between the number of animals with positive contrast flow through the construct and the total number of animals within each experimental group. Within the PMA-coated group, 4 animals that had clinical evidence of patency (positive pulses) were survived up to 12 weeks to evaluate longer term mechanical properties and remodelling. One of these animals was survived up to 24 weeks as preliminary assessment of scaffold performance over an extended period where material degradation might be expected to occur. Table 1 details the number of animals from each experimental group dedicated to each time point.

Gross pathology and histological assessment

Immediately following fluoroscopic assessment, the grafts were harvested along with approximately 5 mm of native aorta at each anastomosis and stored in saline until testing. All the specimens were observed in order to detect signs of infection. Specimens dedicated to histological examination were cut in the central portion of the graft and their lumen was observed at 10× under a zoom stereomicroscope (SMZ660, Nikon Instruments Inc., Melville, NY). Specimens were then fixed in 10% formalin for 1 h and immersed in 30% sucrose solution for 24 hours at 4°C before standard paraffin embedding and sectioning (section thickness = 5 μm). Masson's trichrome, picrosirius red, and van Gieson staining were all performed following standard histological protocols and slides were observed and imaged with bright field microscopy. Picrosirius red stained slides were observed between two polarized lenses in a totally occlusive configuration (90°) to detect birefringency. All histological images were taken with an Eclipse E600 microscope (Nikon Instruments Inc., Melville, NY) equipped with a digital color CCD camera (Model 2.3.1, Diagnostic Instruments Inc., Sterling Heights, MI).

Electron and fluorescence microscopy

Dedicated samples underwent SEM analysis to visualize of the luminal surface and the transition between native aorta and graft. Specimens were fixed and observed following the same protocol and using the same systems previously described for the platelet adhesion assessment.

The scaffolds dedicated to immunohistochemical analysis were fixed in 4% paraformaldehyde for 1 hour and then stored in 30% sucrose solution overnight. The specimens were then embedded in tissue freezing medium (TBS, Triangle Biomedical Sciences, Durham, NC) and sectioned (10 μm thick) with a cryostat. Sections were permeabilized in Triton-X-100 solution for 15 min. Non-specific antibody binding was

blocked by incubating the samples for 45 min with 2% bovine serum albumin (BSA, Fraction V, Sigma) in PBS. The samples were subsequently incubated at room temperature with the primary antibodies (smooth muscle α actin (α-SMA, 1:500, Chemicon, Temecula, CA) and von Willebrand factor (vWF, 1:200, Dako, Carpinteria, CA) diluted in blocking solution for 60 min in a moist chamber to prevent drying of the samples. Unbound primary antibody was removed by subsequent washes in rinsing solution (0.5% BSA + 0.15% glycine in PBS). The samples were then incubated with a Cy3-conjugated secondary antibody (1:500, Sigma–Aldrich, St. Louis, MO) for 1 hour at room temperature and rinsed several times with rinsing solution. Samples were counter-stained with DAPI (bisbenzimide, Sigma) for 1 min and then washed three times with rinsing solution. The sections were observed with epifluorescence microscopy (Eclipse E600, Nikon Instruments Inc., Melville, NY).

Statistical methods

Statistical analyses were performed using SPSS software (v.15, SPSS Inc., Chicago, IL). All datasets were tested for normality with the Shapiro-Wilk test. Comparison of the mean values of different data sets was performed using either a one-way ANOVA for multiple data sets or a Student's t-test for individual comparisons. Post hoc analyses for ANOVA utilized the Bonferroni test. Patency rate was compared with non-parametric values using the exact Fisher test. All measures are presented as mean ± standard deviation. A confidence interval greater than 95% was considered significant ($p<0.05$).

Results

Morphological assessment

The tubular scaffolds grossly appeared smooth and without macroscopic defects following electrospinning (see Fig. 2-A/B). Electron microscopy revealed a circumferentially-uniform wall thickness of approximately 150 μm (Fig. 2-C). The diameter of the electrospun fibers was approximately 1 μm (Fig. 2-D). The PMA coated scaffolds appeared to have a similar luminal surface compared to the bare PEUU (data not shown).

In vitro platelet adhesion assessment

A marked reduction in platelet deposition for the PMA-coated group compared to the bare ES-PEUU surfaces was observed following ovine blood contact *in* vitro. The surface of the ES-PEUU was populated by frequent thrombi comprised of activated and aggregated platelets (Fig. 3-A), while the PMA-coated ES-PEUU had minimal platelet deposition, with randomly observed individual platelets or occasional groupings of few platelets (Fig. 3-B). Image-based platelet counting demonstrated an almost a 10-fold decrease in adherent platelet numbers for the PMA group relative to the uncoated group ($p = 0.0018$) (Fig. 3-C).

In vivo performance

Both the uncoated and the PMA-coated grafts were pliable, non-tacky, and simple to handle and suture during the procedure without showing any detectable difference as a result of the surface modification process. The size and thickness of the graft closely matched the native rat abdominal aorta. The 10-0 stitches could effectively approximate and retain the edges of the graft and aorta resulting in well sealed anastomoses (Fig. 4). The graft also exhibited good visual and tactile pulsatility upon implantation.

The patency of the grafts was easily predicted before euthanasia by manual detection of the pulse immediately distal to the graft location (*i.e.*, iliac bifurcation), and confirmed with fluoroscopy. Generally, non-patent grafts resulted in lack of a detectable pulse, and showed an interruption in the contrast media at the level of the proximal anastomosis, followed by a

late perfusion of the iliac arteries due to contralateral circulation (Fig. 5-A). Patent grafts had a clearly detectable pulse and showed smooth contrast media run-off through the iliac arteries (Fig. 5-B).

At the primary time point of 8 weeks, eleven out of twelve rats in the PMA-coated ES-PEUU graft group showed positive graft flow, resulting in a patency rate of 92% with no signs of ischemia in any of the animals (i.e., seven out of eight animals sacrificed at the 8 week time point combined with the four animals that had clinical evidence of patency and that were extended to longer time points). This result was significantly different when compared to six out of fifteen (40%) ($p=0.014$) with positive flow in the non-coated group, where five animals showed signs of gross ischemia. None of the scaffolds showed signs of an untoward acute inflammatory response or infection. Fluoroscopy showed no signs of aneurysmal dilation or mechanical failure.

Gross morphology and histological assessment

Gross pathological and histological assessment showed two basic modalities of failure for the non-coated grafts: either acute thrombosis (Fig. 5-C and Fig. 6-A), representing about 90% of the obstructed grafts, or intimal hyperplasia (Fig. 6-B). All the PMA-coated grafts (except for the one obstructed at 8 weeks which showed signs of thrombosis) showed a white, glistening lumen (Fig. 5-D) consisting of a multi-layered, collagenous tissue of approximately 50 μm in thickness adherent to the inner surface of the grafts (Fig. 6-C/D and Fig. 7-A/D). Picrosirius red staining confirmed the sub-luminal presence of collagen, and demonstrated a structurally organized luminal layer comprised of deposited collagen fibers oriented circumferentially (Fig. 7-B). Van Gieson staining also revealed the presence of elastin extending radially from the lumen to about 1/3 of the tissue thickness along the circumference of the neo-luminal tissue. The electrospun PMA-coated scaffold did not show significant signs of biological infiltration or remodelling (within the scaffold wall) during the first 24 weeks *in vivo* (Fig. 8). Some of the grafts showed signs of delamination occurring approximately between the outer third of the thickness and the rest of the graft for all the timepoints (Figs.6-A/C and 8-B/C/D).

Examining PMA-coated grafts with electron microscopy revealed no signs of stricture at the anastomotic level (Fig. 9-A), and a good integration between the graft and perivascular tissues (Fig. 9-B). A smooth cellular lining with cobblestone morphology and orientation in the direction of blood flow was consistently shown in the luminal layer (Fig. 9-C). Immunohistochemistry detected a positive expression of α-SMA throughout the thickness of the newly-formed luminal layer (Fig. 10-A). This expression was consistent along the length and the circumference of the scaffolds. A positive signal for von-Willebrand factor was also found on the luminal surface (Fig. 10-B), providing further evidence of endothelial cell lining suggested by the cellular morphology seen in electron micrographs. These observations were consistent along the length and circumference of the scaffold.

The coating process did not affect the mechanical properties of the bare ES-PEUU (data not shown); therefore mechanical data were compared at different time points (only patent scaffolds were tested) disregarding whether the measured scaffold was coated or not. The scaffolds prior to implantation exhibited lower compliances than native rat aortas ($14.2\pm1.1\times10^{-4}$ $mmHg^{-1}$ versus $4.5\pm2.0\times10^{-4}$ $mmHg^{-1}$, $p=0.011$, $n=5$); however, 4 weeks after implantation the compliance increased to values comparable to native tissues. During the following 8 weeks a significant decrease in compliance was detected (Fig. 11-A). The strength and stretch at failure for the PEUU scaffolds prior to implantation were significantly higher than those of native rat aortas (Fig. 11-B/C); however, following implantation and remodelling, both strength and stretch at failure were statistically equivalent to native values.

Discussion

The scaffold represents a critical component in the vascular tissue engineering paradigm. Primary scaffold design requirements include the ability to function as a substrate for tissue remodeling and regeneration, the strength to withstand physiologic arterial conditions over extended periods of time, and the basic blood biocompatibility to resist thrombus formation. Throughout the past several decades many endeavors have been made to develop mechanically and functionally sound scaffolds for vascular tissue engineering to replace or bypass portions of the arterial circulation. Two major approaches have been explored for this purpose, either the incorporation of cells into or onto scaffolds with or without tissue culture in a bioreactor prior to implantation, or the use of acellular scaffolds with properties suitable for *in vivo* remodeling. The second approach has the inherent advantage of offering a readily available scaffold for implantation without the time, cost and potential regulatory implications related to cell sourcing.

Several materials have been used for acellular vascular approaches spanning from decellularized biological tissues to synthetic materials with or without surface functionalization. Decellularized vascular conduits from humans or animals including small diameter veins or arteries have been used with variable levels of success in preclinical studies in small [27], and large animal models [28]. Biologic materials including decellularized tissues tend to offer good initial matching of mechanical properties but high degrees of variability; furthermore, incomplete removal of exogenous materials has been attributed to severe immunological reactions in early human clinical trials [29], and thus these scaffolds, while clearly promising, require significant care in their preparation and characterization. Synthetic scaffolds have the attractive feature of offering tunable and reproducible properties. The most commonly used aliphatic polyesters such as poly(glycolic acid), poly(L-lactic acid), and their copolymers are generally much stiffer than native soft tissues and under some conditions can induce a transient inflammatory response due to the acidity of their degradation products [30]. Synthetic acellular small-diameter vascular conduits have been used in several recent *in vivo* animal studies. Pektoc *et al.* has shown improved patency and endothelialization in rats for 2 mm inner diameter electrospun polycaprolactone grafts compared to ePTFE controls [31]. Yokota *et al.* have implanted in dogs 4 mm-diameter compound grafts made of collagen, polyglycolic acid, and poly-L-lactic acid showing excellent *in situ* tissue regeneration and patency rates [7].

The PEUU used in this study has been shown to be cytocompatible, yield non-toxic degradation products, and to be processable into scaffolds using a variety of techniques [21, 23, 32]. ES-PEUU has been also shown to possess micron and sub-micron fibrous architecture and mechanical properties similar to those of native elastic extracellular matrix [33]. Recent *in vivo* studies showed that this material did not produce a detrimental host inflammatory response due to its degradation products but rather fostered functional remodeling [34, 35]. We have recently reported on the *in vivo* results obtained with acellular, electrospun biodegradable small-diameter vascular grafts based on a blend of PEUU and a phospholipid poly(2-methacryloyloxyethyl phosphorylcholine-co-methacryloyloxyethyl butylurethane) that has some similarities to the surface-modifying polymer used in the current study [36]. These scaffolds, which incorporated the phopholipid-mimic polymer throughout their structure showed significant reduction in platelet and smooth muscle cell adhesion *in vitro*, and increased patency rates in the rat model *in vivo*.

The surface-treated ES-PEUU scaffolds developed in this study had no apparent differences in pore and fiber size, porosity, or wall thickness compared to untreated PEUU control. Functionally, the treatment resulted in a significant reduction in platelet adhesion *in vitro*

(Fig. 3). The non-thrombogenic properties of the PMA coating were confirmed *in vivo*, with significantly higher patency rates at 8 weeks between the ES-PEUU and the PMA-treated group. This effect was attributed to the MPC structure attached to the luminal surface and its zwitterionic similarities to the surface presented by the outer layer of cell membrane. A substantial literature exists on MPC-based polymers applied to a variety of surfaces to reduce protein adsorption and anzymatic pathway activation, as well as to inhibit cellular adhesion processes [37, 38]. It would generally be expected that each of these activities related to inhibiting blood protein adhesion and activation would act to reduce surface thrombogenicity as was seen in this study.

Histologically, the scaffolds demonstrated the propensity to provide an environment suitable for neo-vascular tissue formation. The neointimal tissue had structural and phenotypic similarities with native arterial tissue as demonstrated by the presence of aligned collagen and elastin (Figs.7–8), and by the immunohistochemical markers consistent with smooth muscle and endothelial cells (Fig. 10), respectively. However, the lack of significant cellular infiltration into the scaffold, and the preserved scaffold structure found at each time point including the single animal brought to 24 weeks (Fig. 8), suggest that this scaffold possesses a very slow degradation rate *in vivo*. We believe that the structural features of the ES-PEUU scaffolds including the small pore size of the matrix obtained by electrospinning, potentially the orientation of the PEUU polymer within the fibers to increase crystallinity, as well as the thickness of the scaffold may have all contributed to slowing cellular infiltration and the degradation process of PEUU beyond that seen in other locations in the rat with alternative processing [39]. Our recent report detailing the results obtained in a rat model with a bilayered vascular scaffold including an external layer of electrospun PEUU [26] suggests extensive degradation after 8 weeks for the electrospun portion of the scaffold [34]. Longer *in vivo* studies are required to evaluate the capacity of the PMA-coated ES-PEUU scaffold to be effectively replaced by new functional tissue upon complete scaffold degradation and long term propensity for aneurismal dilatation cannot dismissed from the data collected here. Some of the scaffolds used in this study exhibited a single delamination across the wall thickness, as observed in Figs.6 and 8. The presence of neotissue infiltration within the delaminated areas in some of the samples is suggestive of a processing issue occurring during the electrospinning process. Excessive fiber dryness, as might occur when the polymer flow rate is low and the distance between nozzle and target is high, may have led to poor “solvent bonding” between fibers and thus delamination. In some cases the histological preparation of the sample might have also fostered further separation of the layers. The observed phenomenon, although clearly not desirable, does not seem to affect either the remodeling of the grafts or their mechanical properties.

For the implant durations studied here (i.e., 4, 8, 12, and 24 weeks), the scaffolds showed sufficient strength for arterial vascular applications without evidence of dilation or aneurysm formation (Figs.5–8). The scaffolds exhibited physiologically-compatible values of compliance prior to implantation (Fig. 11) when compared with native rat aortas and with previously measured values for human coronary arteries (compliance=$14.1\pm5.9\times10^{-4}$ $mmHg^{-1}$) [40]. The scaffold compliance and strength throughout the 3 measured time points *in vivo* underwent some notable changes (Fig. 11), in particular, an increase in compliance and decrease in strength resulting from the first 4 weeks *in vivo* and the subsequent reduction in compliance. A possible explanation for the increase in compliance could be that the scaffolds during the first weeks of implantation undergo some acute baseline degradation resulting in increased compliance and decreased strength. Hydrolytic cleavage of the connection points between individual electrospun fibers would be expected to reduce the scaffold resistance to distension. Such connection points might be candidates for degradation given their small volume. The subsequent process of neo-tissue formation both on the luminal and abluminal sides of the scaffolds likely then contributed to the decrease in

compliance as these biological components acted to increase overall conduit stiffness. While compliance measurements were conducted on the whole explanted grafts, uniaxial testing was performed on very small rings cut from the graft which could lose the internal and external neo-tissue formation and therefore, their mechanical contribution. This loss of potential load bearing components in processing prior to testing may have contributed to the loss of strength seen in the data. In general, the very slow degradation for the ES-PEUU scaffolds and the lack of tissue infiltration throughout the tightly linked fibrillar scaffold in the time periods examined prevent confirmation that the approach of this study would lead to neo-tissue formation that is mechanically robust enough to function as a stable arterial replacement. While the histological aspects of the forming neointimal tissue are encouraging, longer time points along with a thorough degradation study for the specific scaffold would need to be examined, or a more rapidly degrading substrate might be considered.

A small-diameter vascular graft luminally modified with a phospholipid mimicking copolymer exhibited excellent non-thrombogenic properties *in vitro* and *in vivo*, and mechanical properties compatible with native arterial conduits. Following *in vivo* remodeling, the grafts showed a neo-intimal tissue formation that exhibited both smooth muscle and endothelial markers as well as oriented collagen and elastin deposition. These features might represent a step toward future clinical translation of an “off-the-shelf” vascular graft enabling vascular regeneration.

Acknowledgments

The authors gratefully acknowledge the financial support of the United States National Institutes of Health through BRP grant number R01 HL069368 (to Drs. Wagner and Vorp). The authors would like to express thanks to Prof. Kazuhiko Ishihara, The University of Tokyo who kindly provided the PMA copolymer.

References

1. Weintraub WS, Jones EL, Craver JM, Guyton RA. Frequency of repeat coronary bypass or coronary angioplasty after coronary artery bypass surgery using saphenous venous grafts. Am J Cardiol. 1994 Jan; 73(2):103–112. [PubMed: 8296729]
2. Xue L, Greisler HP. Biomaterials in the development and future of vascular grafts. J Vasc Surg. 2003 Feb; 37(2):472–480. [PubMed: 12563226]
3. Roeder R, Wolfe J, Lianakis N, Hinson T, Geddes LA, Obermiller J. Compliance, elastic modulus, and burst pressure of small-intestine submucosa (SIS), small-diameter vascular grafts. J Biomed Mater Res. 1999 Oct; 47(1):65–70. [PubMed: 10400882]
4. McFetridge PS, Daniel JW, Bodamyali T, Horrocks M, Chaudhuri JB. Preparation of porcine carotid arteries for vascular tissue engineering applications. J Biomed Mater Res A. 2004 Aug 1; 70(2):224–234. [PubMed: 15227667]
5. Zavan B, Vindigni V, Lepidi S, Iacopetti I, Avruscio G, Abatangelo G, et al. Neoarteries grown in vivo using a tissue-engineered hyaluronan-based scaffold. FASEB J. 2008 Apr 2.
6. Berglund JD, Nerem RM, Sambanis A. Incorporation of intact elastin scaffolds in tissue-engineered collagen-based vascular grafts. Tissue Eng. 2004 Sep-Oct; 10(9–10):1526–1535. [PubMed: 15588412]
7. Yokota T, Ichikawa H, Matsumiya G, Kuratani T, Sakaguchi T, Iwai S, et al. In situ tissue regeneration using a novel tissue-engineered, small-caliber vascular graft without cell seeding. J Thorac Cardiovasc Surg. 2008 Oct; 136(4):900–907. [PubMed: 18954628]
8. Naito Y, Imai Y, Shin’oka T, Kashiwagi J, Aoki M, Watanabe M, et al. Successful clinical application of tissue-engineered graft for extracardiac Fontan operation. J Thorac Cardiovasc Surg. 2003 Feb; 125(2):419–420. [PubMed: 12579118]

9. van der Lei B, Wildevuur CR. From a synthetic, microporous, compliant, biodegradable small-caliber vascular graft to a new artery. Thorac Cardiovasc Surg. 1989 Dec; 37(6):337–347. [PubMed: 2694440]
10. Galletti G, Gogolewski S, Ussia G, Farruggia F. Long-term patency of regenerated neoaortic wall following the implant of a fully biodegradable polyurethane prosthesis: experimental lipid diet model in pigs. Ann Vasc Surg. 1989 Jul; 3(3):236–243. [PubMed: 2775639]
11. L'Heureux N, McAllister TN, de la Fuente LM. Tissue-engineered blood vessel for adult arterial revascularization. N Engl J Med. 2007 Oct 4; 357(14):1451–1453. [PubMed: 17914054]
12. Pavcnik D, Obermiller J, Uchida BT, Van Alstine W, Edwards JM, Landry GJ, et al. Angiographic evaluation of carotid artery grafting with prefabricated small-diameter, small-intestinal submucosa grafts in sheep. Cardiovasc Intervent Radiol. 2009 Jan; 32(1):106–113. [PubMed: 18931872]
13. Haruguchi H, Teraoka S. Intimal hyperplasia and hemodynamic factors in arterial bypass and arteriovenous grafts: a review. 2003; 6(4):227–235.
14. Sung HJ, Meredith C, Johnson C, Galis ZS. The effect of scaffold degradation rate on three-dimensional cell growth and angiogenesis. Biomaterials. 2004 Nov; 25(26):5735–5742. [PubMed: 15147819]
15. Woods AM, Rodenberg EJ, Hiles MC, Pavalko FM. Improved biocompatibility of small intestinal submucosa (SIS) following conditioning by human endothelial cells. Biomaterials. 2004 Feb; 25(3):515–525. [PubMed: 14585701]
16. Mann BK, West JL. Cell adhesion peptides alter smooth muscle cell adhesion, proliferation, migration, and matrix protein synthesis on modified surfaces and in polymer scaffolds. Journal of Biomedical Materials Research. 2002 Apr; 60(1):86–93. [PubMed: 11835163]
17. Krijgsman B, Seifalian AM, Salacinski HJ, Tai NR, Punshon G, Fuller BJ, et al. An assessment of covalent grafting of RGD peptides to the surface of a compliant poly(carbonate-urea)urethane vascular conduit versus conventional biological coatings: its role in enhancing cellular retention. Tissue Eng. 2002 Aug; 8(4):673–680. [PubMed: 12202006]
18. Garcia-Honduvilla N, Dominguez B, Pascual G, Escudero C, Minguela F, Bellon JM, et al. Viability of engineered vessels as arterial substitutes. Ann Vasc Surg. 2008 Mar; 22(2):255–265. [PubMed: 18346580]
19. Yoneyama T, Sugihara K, Ishihara K, Iwasaki Y, Nakabayashi N. The vascular prosthesis without pseudointima prepared by antithrombogenic phospholipid polymer. Biomaterials. 2002 Mar; 23(6):1455–1459. [PubMed: 11829441]
20. Kobayashi K, Ohuchi K, Hoshi H, Morimoto N, Iwasaki Y, Takatani S. Segmented polyurethane modified by photopolymerization and cross-linking with 2-methacryloyloxyethyl phosphorylcholine polymer for blood-contacting surfaces of ventricular assist devices. J Artif Organs. 2005; 8(4):237–244. [PubMed: 16362521]
21. Stankus JJ, Guan J, Wagner WR. Fabrication of biodegradable elastomeric scaffolds with sub-micron morphologies. J Biomed Mater Res A. 2004 Sep 15; 70(4):603–614. [PubMed: 15307165]
22. Stankus JJ, Soletti L, Fujimoto K, Hong Y, Vorp DA, Wagner WR. Fabrication of cell microintegrated blood vessel constructs through electrohydrodynamic atomization. Biomaterials. 2007 Jun; 28(17):2738–2746. [PubMed: 17337048]
23. Guan J, Sacks MS, Beckman EJ, Wagner WR. Synthesis, characterization, and cytocompatibility of elastomeric, biodegradable poly(ester-urethane)ureas based on poly(caprolactone) and putrescine. J Biomed Mater Res. 2002 Sep 5; 61(3):493–503. [PubMed: 12115475]
24. Ishihara K, Hanyuda H, Nakabayashi N. Synthesis of phospholipid polymers having a urethane bond in the side chain as coating material on segmented polyurethane and their platelet adhesion-resistant properties. Biomaterials. 1995 Jul; 16(11):873–879. [PubMed: 8527604]
25. Severyn DA, Muluk SC, Vorp DA. The influence of hemodynamics and wall biomechanics on the thrombogenicity of vein segments perfused in vitro. J Surg Res. 2004 Sep; 121(1):31–37. [PubMed: 15313372]
26. Soletti L, Hong Y, Guan J, Stankus JJ, El-Kurdi MS, Wagner WR, et al. A bilayered elastomeric scaffold for tissue engineering of small diameter vascular grafts. Acta Biomater. 2009 Jun 18.

27. Gui L, Muto A, Chan SA, Breuer CK, Niklason LE. Development of decellularized human umbilical arteries as small-diameter vascular grafts. Tissue Eng Part A. 2009 Sep; 15(9):2665–2676. [PubMed: 19207043]

28. Cho SW, Lim JE, Chu HS, Hyun HJ, Choi CY, Hwang KC, et al. Enhancement of in vivo endothelialization of tissue-engineered vascular grafts by granulocyte colony-stimulating factor. J Biomed Mater Res A. 2006 Feb; 76(2):252–263. [PubMed: 16265638]

29. Simon P, Kasimir MT, Seebacher G, Weigel G, Ullrich R, Salzer-Muhar U, et al. Early failure of the tissue engineered porcine heart valve SYNERGRAFT in pediatric patients. Eur J Cardiothorac Surg. 2003 Jun; 23(6):1002–1006. discussion 1006. [PubMed: 12829079]

30. Yang S, Leong KF, Du Z, Chua CK. The design of scaffolds for use in tissue engineering. Part I. Traditional factors. Tissue Eng. 2001 Dec; 7(6):679–689. [PubMed: 11749726]

31. Pektok E, Nottelet B, Tille JC, Gurny R, Kalangos A, Moeller M, et al. Degradation and healing characteristics of small-diameter poly(epsilon-caprolactone) vascular grafts in the rat systemic arterial circulation. Circulation. 2008 Dec 9; 118(24):2563–2570. [PubMed: 19029464]

32. Guan J, Fujimoto KL, Sacks MS, Wagner WR. Preparation and characterization of highly porous, biodegradable polyurethane scaffolds for soft tissue applications. Biomaterials. 2005 Jun; 26(18): 3961–3971. [PubMed: 15626443]

33. Courtney T, Sacks MS, Stankus J, Guan J, Wagner WR. Design and analysis of tissue engineering scaffolds that mimic soft tissue mechanical anisotropy. Biomaterials. 2006 Jul; 27(19):3631–3638. [PubMed: 16545867]

34. Nieponice A, Soletti L, Guan J, Hong Y, Maul T, Gharaibeh B, et al. In-vivo Assessment of a Tissue-engineered Vascular Graft Combining a Biodegradable Elastomeric Scaffold and Muscle-Derived Stem Cells in a Rat Model. Tissue Eng Part A. In press, available online.

35. Fujimoto KL, Tobita K, Merryman WD, Guan J, Momoi N, Stolz DB, et al. An elastic, biodegradable cardiac patch induces contractile smooth muscle and improves cardiac remodeling and function in subacute myocardial infarction. J Am Coll Cardiol. 2007 Jun 12; 49(23):2292–2300. [PubMed: 17560295]

36. Hong Y, Ye SH, Nieponice A, Soletti L, Vorp DA, Wagner WR. A small diameter, fibrous vascular conduit generated from a poly(ester urethane)urea and phospholipid polymer blend. Biomaterials. 2009 May; 30(13):2457–2467. [PubMed: 19181378]

37. Nakabayashi N, Williams DF. Preparation of non-thrombogenic materials using 2-methacryloyloxyethyl phosphorylcholine. Biomaterials. 2003 Jun; 24(13):2431–2435. [PubMed: 12699681]

38. Ishihara K, Nomura H, Mihara T, Kurita K, Iwasaki Y, Nakabayashi N. Why do phospholipid polymers reduce protein adsorption? J Biomed Mater Res. 1998 Feb; 39(2):323–330. [PubMed: 9457564]

39. Fujimoto KL, Guan J, Oshima H, Sakai T, Wagner WR. In vivo evaluation of a porous, elastic, biodegradable patch for reconstructive cardiac procedures. Ann Thorac Surg. 2007 Feb; 83(2): 648–654. [PubMed: 17258002]

40. Tajaddini A, Kilpatrick DL, Schoenhagen P, Tuzcu EM, Lieber M, Vince DG. Impact of age and hyperglycemia on the mechanical behavior of intact human coronary arteries: an ex vivo intravascular ultrasound study. Am J Physiol Heart Circ Physiol. 2005 Jan; 288(1):H250–255. [PubMed: 15331362]

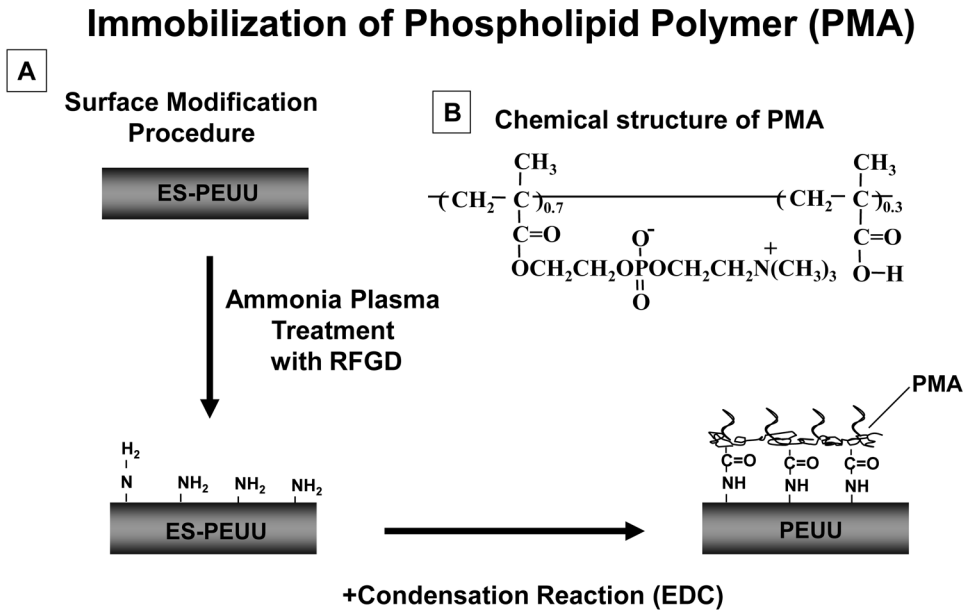

Figure 1.

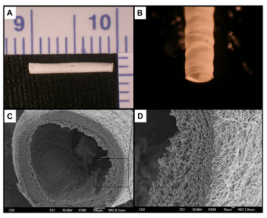

Figure 2.

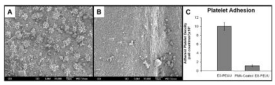

Figure 3.

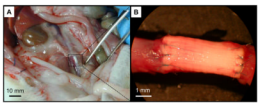

Figure 4.

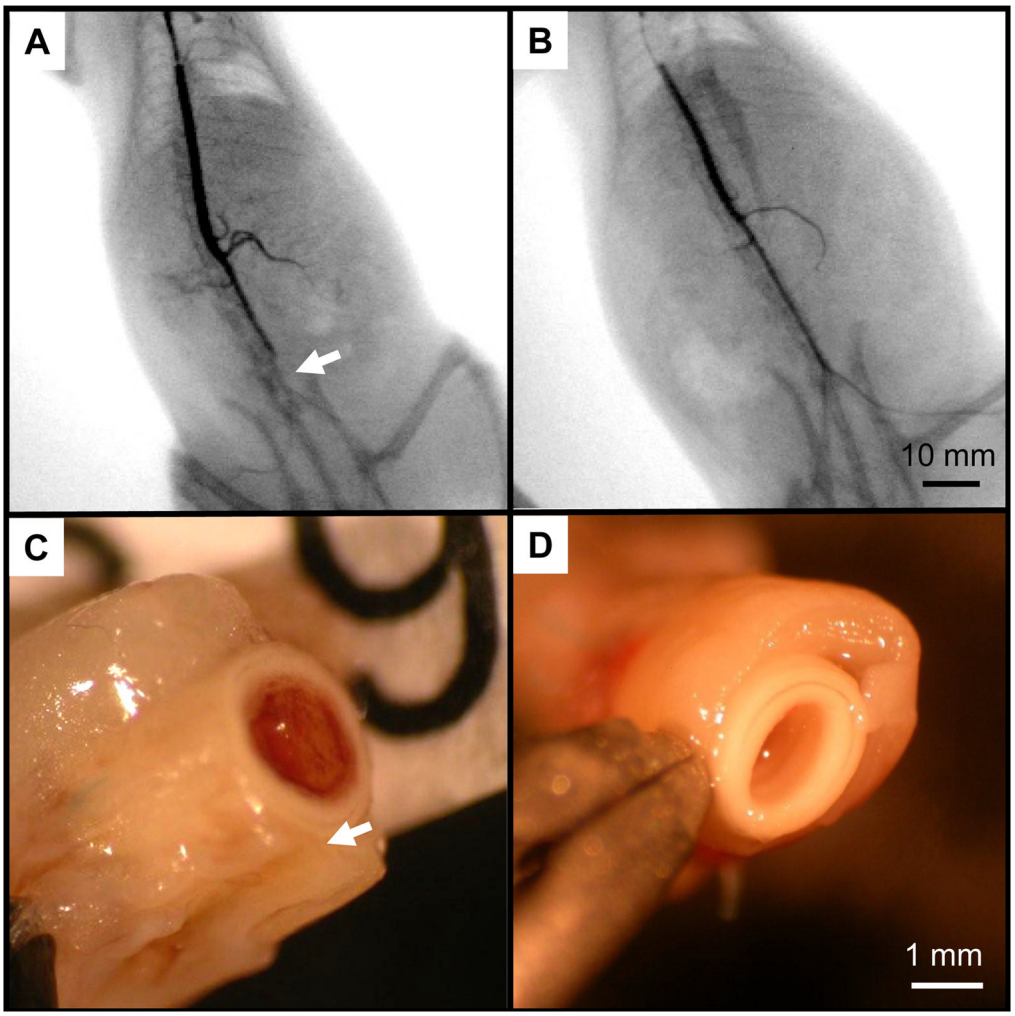

Figure 5.

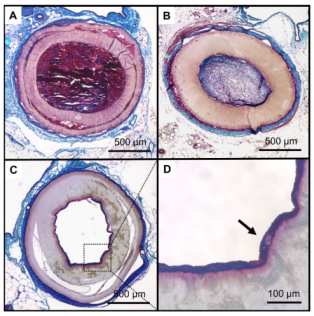

Figure 6.

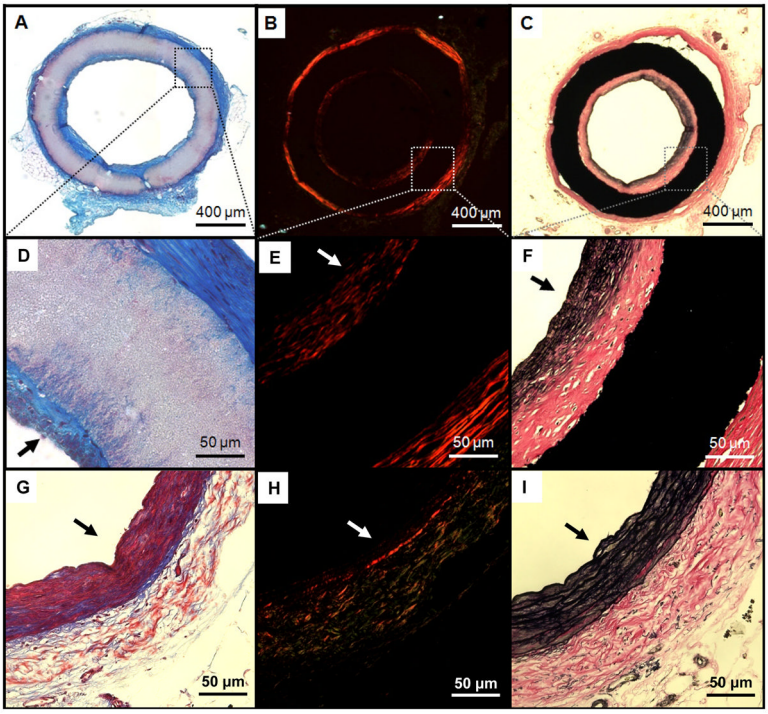

Figure 7.

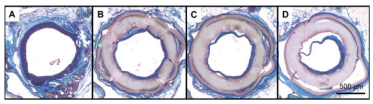

Figure 8.

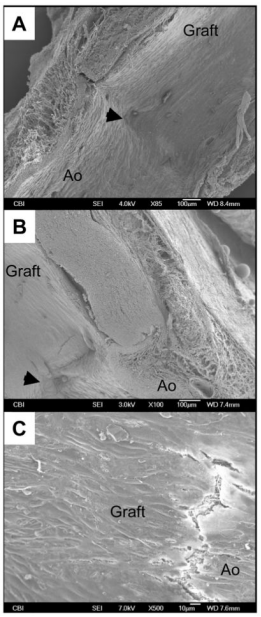

Figure 9.

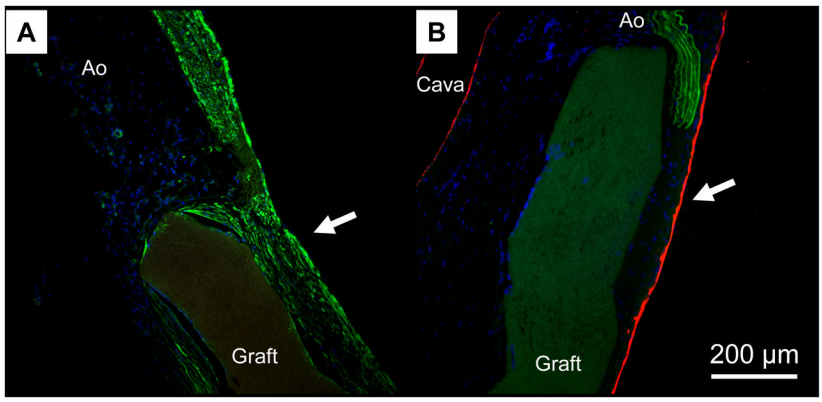

Figure 10.

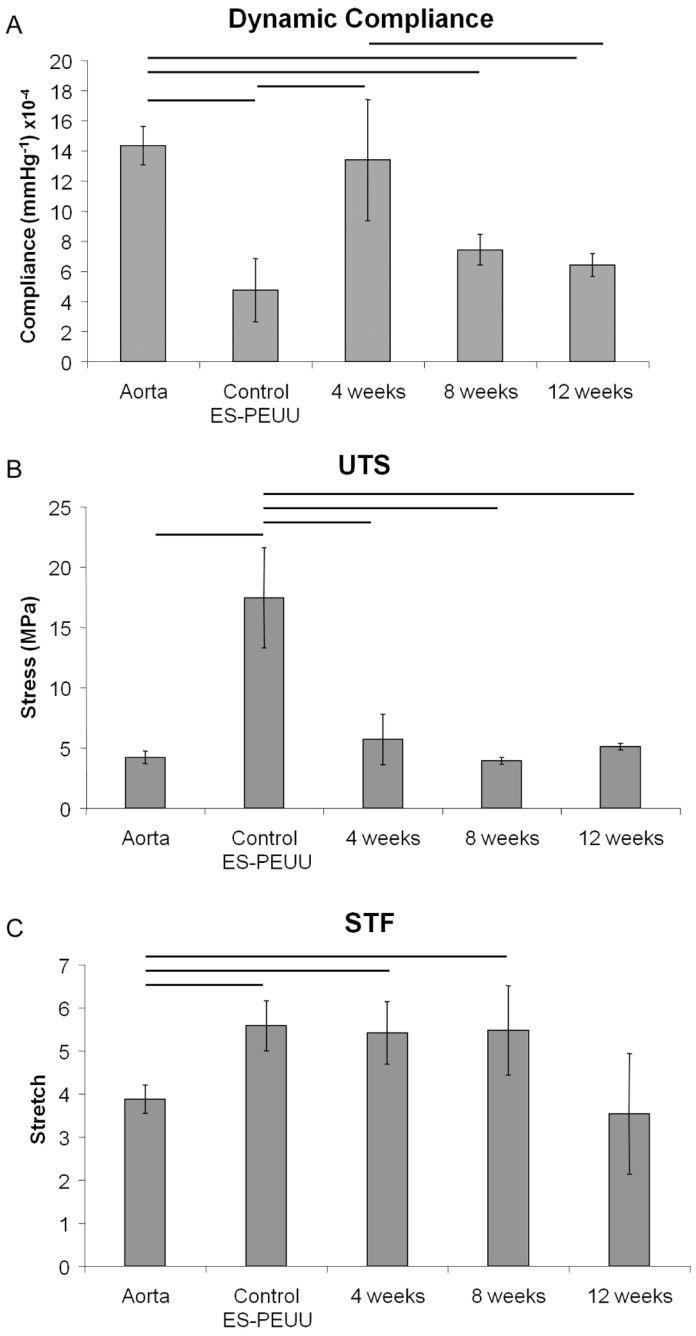

Figure 11.

Table 1

Number of animals used in each experimental group

	4 weeks	8 weeks	12 weeks	24 weeks
Uncoated	n=10	n=15	n/a	n/a
PMA-Coated	n/a	n=8	n=3	n=1